On the Analysis of Noise and Interference in Instantaneously Companding Signal Processors

László Tóth, Yannis P. Tsividis, *Fellow, IEEE*, and Nagendra Krishnapura

***Abstract*—Certain issues in the analysis of the effects of noise and interference in instantaneously companding signal processors is discussed. Important differences from the analysis and effects encountered in conventional signal processors are pointed out, and are illustrated by deriving analytical results for deterministic small interference and stationary random noise in a first-order instantaneously companding filter. The theoretical calculations are successfully compared to experimental results.**

***Index Terms*—Companding, noise, log-domain filters.**

I. Introduction

COMPANDING (compressing/expanding) signal processing has been proposed as a way of maintaining adequate dynamic range in integrated circuits with low power supply voltage [1], [2]. Companding is also present, to a small or large extent, in circuits proposed with a different purpose in mind, namely to achieve linear tunable signal processing using nonlinear circuit elements [3]–[5]. Such circuits will also be referred to as "companding" in this paper. Although such circuits perform linear operations on the input signal, they are nonlinear from internal points to the output. This fact leads to unusual behavior with respect to noise and interference [6]. In this paper, a preliminary investigation of this behavior is undertaken. The inadequacy of classical analysis techniques, commonly applied to conventional signal processors, are pointed out, and methods for the analysis of noise and interference in companding signal processors are discussed. The paper emphasizes instantaneously companding signal processors. However, the techniques considered are relevant to the analysis of syllabically companding signal processors as well [6], as will be discussed.

Throughout this paper, a first-order system is used as an example. This is done both in order not to allow complexity to obscure the results, and because integrators are the dominant building blocks in high-order filter structures. The application of the techniques discussed to higher order structures is, in principle, straightforward, albeit lengthy, necessitating the use of appropriate computer programs.

We consider a prototype signal processor with linear input–output behavior, characterized by a transfer function of the form:

$$H(s) = \frac{k}{s+a} \tag{1}$$

where k and a are known constants. This prototype can be implemented as in Fig. 1. The state variable description of this system is:

$$\dot{x} = -ax + ku \tag{2}$$

$$y = x \tag{3}$$

where x is the state variable, and $\dot{x}$ is its time derivative. We now consider a system with the same input–output behavior, but with a state variable v, which is related to x by [2], [5]

$$x = f(v) \tag{4}$$

where $f(v)$ is a monotonic function with continuous nonzero derivative for all v. Using (4) in (2) and (3) we obtain

$$\frac{d}{dt} f(v) = -af(v) + ku \tag{5}$$

$$y = f(v) \tag{6}$$

or, using $(d/dt)f(v) = f'(v)\dot{v}$, where $f'(v)$ is the derivative of $f(v)$ with respect to v:

$$\dot{v} = -a\frac{f(v)}{f'(v)} + \frac{k}{f'(v)}u \tag{7}$$

$$y = f(v). \tag{8}$$

An implementation of these equations is shown in Fig. 2. In this system, the square blocks represent memoryless nonlinearities, whereas the triangle is a gain block. The behavior between u and y is linear and is still described by (2) and (3) [2], [5]. In a log-domain circuit [2], [3], [5], $f(\cdot)$ is an exponential, and u, y are currents, leading to efficient implementation with bipolar transistors.

We now consider the effects of small additive interference and noise signals (referred to jointly as "noise") on this system. It is obvious that noise at the output is simply added to y, and

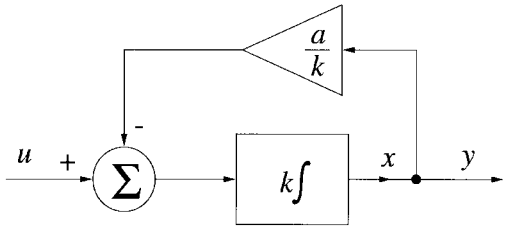

Fig. 1. Linear first-order system.

Manuscript received June 2, 1997; revised November 11, 1997. This paper was recommended by Associate Editor L. A. Akers.

L. Tóth is with the Communications Systems Research Laboratory, Lucent Technologies, Bell Labs Innovations, Murray Hill, NJ 07974 USA.

Y. P. Tsividis and N. Krishnapura is with the Microelectronic Circuits and Systems Laboratory, Department of Electrical Engineering, Columbia University, New York, NY 10027 USA.

Publisher Item Identifier S 1057-7130(98)06697-X.

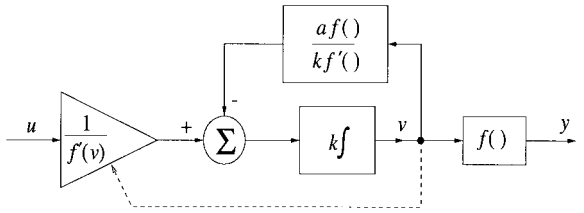

Fig. 2. Input–output linear first-order system.

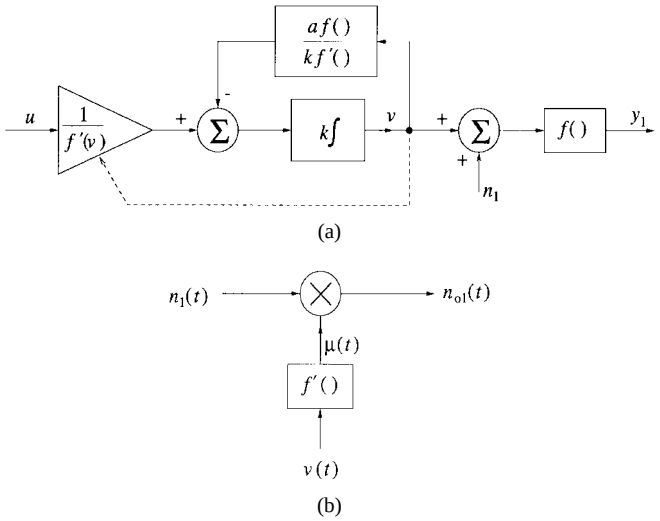

Fig. 3. (a) Memoryless processing of interference. (b) Equivalent small-signal system.

that noise at the input is processed along with the signal by the transfer function in (1). However, noise at internal points undergoes nonlinear signal processing. This is demonstrated by considering two representative cases in the following section.

II. Time Response to Small Interference and Noise at Internal Points

A. Memoryless Processing of Small Interference and Noise

Consider the additive noise n_1 shown in Fig. 3(a). This noise source does not affect anything to the left of it, so v is not influenced by it. The output is

$$y_1 = f(v + n_1). \tag{9}$$

Assuming that n_1 is sufficiently small, we can use the approximation

$$y_1 = f(v) + f'(v)n_1. \tag{10}$$

The amount by which this differs from the output y of the noiseless system in (8), is defined as the output noise n_{o1}. From (8) and (10)

$$n_{o1}(t) = y_1(t) - y(t) = \mu(t)n_1(t) \tag{11}$$

where

$$\mu(t) = f'(v(t)). \tag{12}$$

A straightforward way to obtain $\mu(t)$ for a given $u(t)$ is to compute $y(t)$ using the transfer function in (1), and then use (3) and (4) to obtain $v(t) = f^{-1}(x(t)) = f^{-1}(y(t))$. Substituting $v(t)$ into $f'(v)$ gives $\mu(t)$ according to (12).

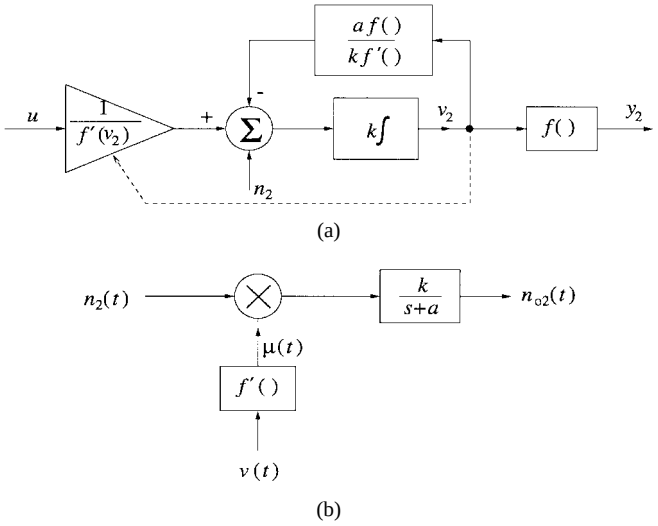

Fig. 4. (a) Interference processing involving elements with memory. (b) Equivalent small-signal system.

The result in (11) can be represented by the equivalent small-signal noise system in Fig. 3(b). As seen, the noise n_1 is processed by a linear time-varying (LTV) memoryless system, with a time-varying gain dependent on $v(t)$. A relevant characterization of an LTV system involves its response to a delayed delta function $\delta(t-\tau)$ [7]. For the system in Fig. 3(b), replacing $n_1(t)$ by $\delta(t-\tau)$, and denoting the resulting output by $h_1(t, \tau)$, we have

$$h_1(t, \tau) = \mu(t)\delta(t-\tau) \tag{13}$$

$$= \mu(\tau)\delta(t-\tau). \tag{14}$$

The Fourier transform of this response with t as the "time" variable is

$$H_1(\omega, \tau) = \mu(\tau)e^{-j\omega\tau}. \tag{15}$$

Such transforms are used in the analysis of LTV systems [7] and linear periodically time-varying (LPTV) systems [8]. For a known $n_1(t)$, one can obtain $n_{o1}(t)$ by using basic techniques of Fourier transformation [7], [8]. This would be useful, for example, for calculating the effect of a small interfering signal finding its way to the input of the $f(\cdot)$ block in Fig. 3(a), coming from another part of the chip containing the processor under study.

B. Interference and Noise Processing Involving Elements with Memory

Consider now the additive noise n_2 at the summer, as shown in Fig. 4(a). This can represent external interference, or the output noise of the left-hand block, or the output noise of the upper block, or the equivalent input referred noise of the integrator. Now the state variable $v_2(t)$ *is* affected, and will be different from $v(t)$ in Fig. 2. Writing the state equations for Fig. 4(a) we have

$$\dot{v_2} = -a\frac{f(v_2)}{f'(v_2)} + \frac{k}{f'(v_2)}u + kn_2 \tag{16}$$

$$y_2 = f(v_2) \tag{17}$$

or, multiplying both sides of (16) by $f'(v_2)$ and using $f'(v_2)\dot{v}_2 = (d/dt)f(v_2)$

$$\frac{d}{dt}f(v_2) = -af(v_2) + ku + kf'(v_2)n_2 \tag{18}$$

$$y_2 = f(v_2). \tag{19}$$

Subtracting (5) and (6) from (18) and (19), respectively, we obtain

$$\frac{d}{dt}(f(v_2) - f(v)) = -a(f(v_2) - f(v)) + kf'(v_2)n_2 \tag{20}$$

$$y_2 - y = f(v_2) - f(v). \tag{21}$$

Define the output noise (relative to the noiseless system in Fig. 2) as

$$n_{o2} = y_2 - y = f(v_2) - f(v). \tag{22}$$

Replacing $f(v_2) - f(v)$ in (20) by n_{o2} gives:

$$\dot{n}_{o2} = -an_{o2} + kf'(v_2)n_2. \tag{23}$$

Since $f'(v)$ has been assumed continuous, if n_2 is sufficiently small we can replace $f'(v_2)$ by $f'(v)$ in (23). Thus, we have

$$\frac{d}{dt}n_{o2}(t) = -an_{o2}(t) + k\mu(t)n_2(t) \tag{24}$$

where $\mu(t)$ has been defined in (12). The differential equation in (24) is linear with respect to $\mu(t)n_2(t)$, and can be represented by the small-signal noise equivalent system of Fig. 4(b). This is again a LTV system between n_{o2} and n_2. Its response $h_2(t, \tau)$ (at the output n_{o2}) to a delayed delta function $\delta(t-\tau)$ (at the input n_2) is

$$\begin{aligned} h_2(t, \tau) &= (\mu(t)\delta(t-\tau)) * h(t) \\ &= \mu(\tau)(\delta(t-\tau) * h(t)) \\ &= \mu(\tau)h(t-\tau) \end{aligned} \tag{25}$$

where $*$ stands for convolution and $h(t)$ is the impulse response corresponding to $H(s)$ in (1). The Fourier transform of the response $h_2(t, \tau)$ w.r.t. the variable t is

$$H_2(\omega, \tau) = e^{-j\omega\tau}\mu(\tau)H(j\omega). \tag{26}$$

Again, for a known $n_2(t)$ one can use (24)–(26) to analyze the behavior of the system. Our analysis so far has placed no restriction as to the nature of the "noise," other than that its magnitude is small. It can thus be applied, for example, in the evaluation of the signal processor output when the "noise" is deterministic interference. The following section deals with the special case where the "noise" is true random noise.

III. Response to Stationary White Noise in the Presence of a Periodic Input

If n_1 or n_2 is random noise, the evaluation of the output noise can in general be very complicated. We have found explicit expressions under the following two assumptions.:

- the noise is wide-sense stationary and white,[1] with zero mean (an assumption which is not always valid—see below);
- the input $u(t)$ is periodic, and the corresponding noiseless system (Fig. 2) has reached steady state.

In such cases, we can evaluate the output noise power spectral density (PSD) by [8]

$$S_o(\omega) = S_n \frac{1}{T}\int_0^T |H(\omega, \tau)|^2 \, d\tau \tag{27}$$

where S_n is the PSD of the noise excitation, T is the period of the input, and $H(\omega, \tau)$ is the Fourier transform of the response of the corresponding small-signal LPTV system (see Section II) to a shifted delta function $\delta(t-\tau)$.[2]

For the noise source n_1 (see Section II-A) with PSD S_1 we have, using (15) and (27), a corresponding output PSD of

$$S_{o1}(\omega) = \eta S_1 \tag{28}$$

where

$$\eta = \frac{1}{T}\int_0^T \mu^2(\tau)\, d\tau. \tag{29}$$

For the noise source n_2 (see Section II-B), assuming a PSD S_2 we have, using (26) and (27), a corresponding output PSD of

$$S_{o2}(\omega) = \eta|H(\omega)|^2 S_2 \tag{30}$$

or, using (1):

$$S_{o2}(\omega) = \eta \frac{k^2}{a^2 + \omega^2} S_2. \tag{31}$$

If n_{o1} and n_{o2} are uncorrelated, their combined effect on the output PSD can be found by adding S_{o1} and S_{o2}. However, if n_{o1} and n_{o2} represent interference, it is likely that they will be correlated.

IV. Discussion

It is clear from the above analysis that companding signal processors respond to interference or noise at internal points, in a manner quite different from conventional processors. The following observations are in order.

1) As is evident from the equivalent systems in Figs. 3(b) and 4(b), small interference or noise finding its way to internal points will be modulated by the signal, and will produce intermodulation components between the input frequencies and the interference or noise frequencies.
2) The amount of output noise or interference *depends on the signal level* [6]. This is evident from the fact that in (28) and (30) the factor η appears. This factor, given by (29), depends on $\mu(t)$ and thus on $v(t)$ through (12); $v(t)$, in turn, depends on the input $u(t)$ as seen in Fig. 2.
3) The amount of output noise or interference *depends on the signal shape*. This is again evident from the dependence of η on $\mu(t)$.
4) If more than one signal is present at the input, the *combined* signal determines the output noise, through $v(t)$ in (12) and (29). The possibility thus exists that

[1] Assuming white noise also serves to keep the discussion simple. Colored (nonwhite) stationary noise sources can be modeled by using appropriate noise-shaping filters, as in, say [9]. After including the noise-shaping filter into the system to be analyzed, one can apply the techniques described in this paper.

[2] The original proof of (27) in [8] assumed Gaussian white noise source, but the same formula can be obtained as a special case of the more general result in [10] (see, e.g., [11]) with general (not necessarily Gaussian) wide-sense stationary white noise.

the noise caused by the presence of a large signal can "drown out" a small signal at the output. This can happen even if the large signal itself is out of band and is thus absent at the output. This is because, at the output of intermediate stages, such a signal might not have been sufficiently rejected, and thus, its large magnitude can increase the noise level at those points and cause the above problem.

In Section III, it was assumed that the noise sources are stationary. The reader is cautioned that this may not be the case for all noise sources in a companding signal processor. This is because, in contrast to small-signal applications, the devices in a companding signal processor can undergo large signal excursions (if these excursions are slow, they can be viewed as slowly varying bias points; for example, the nonstationarity of bipolar transistor shot noise in such a case is intuitively expected). Such cases cannot be handled in a general way as above, since they are totally dependent on the details of the circuit implementation. Correlations between noise sources (such as those caused, for example, by a common bias string) further complicate the picture. Such cases can be handled, in principle, by incorporating nonstationary noise models as in [9], [13], [15], but the complexity involved makes simulation indispensable. Such simulation cannot be done using conventional small-signal "AC" noise analysis, but instead requires specialized programs [9], [14], [15].

Although this paper focuses on instantaneously companding signal processors, the analysis techniques discussed are relevant to syllabically companding ones too. In fact, from the point of view of noise, such processors can in some cases be treated as LTV systems not approximately as above, but exactly [6]. The noise properties of such processors, though, can depend strongly on the details of circuits outside the main signal path, leading to the "envelope-transient noise" phenomenon [6].

V. Examples

Consider the log-domain circuit in Fig. 5 [2], [16]. The quantity i_{n2} represents a stationary noise current which, for example, can originate in the devices that develop I, or can represent external interference. Assume first that $i_{n2} = 0$. An analysis can be performed [2], [16], [17], assuming all base currents are negligible, and writing Kirchoff's current law for the node "v," and using exponential relations between the base–emitter voltages and the collector currents. This gives equations of the form of (7) and (8), with

$$f(v) = I_s e^{v/V_T} \tag{32}$$

$$k = \frac{I_0}{CV_T} \tag{33}$$

$$a = \frac{I}{CV_T} \tag{34}$$

where I_s is the reverse saturation current of the transistors (assumed the same for all the transistors) and V_T is the "thermal voltage" ($V_T = kT/q$, 26 mV at room temperature).

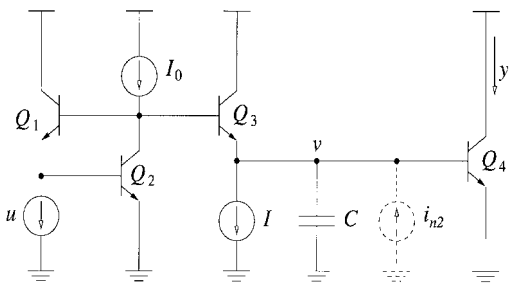

Fig. 5. First-order class-A log-domain circuit.

If $i_{n2} \neq 0$, the equations are in the form of (16), (17) with

$$n_2 = \frac{V_T}{I_0} i_{n2}. \tag{35}$$

Equations (1), (33), and (34) give

$$H(j\omega) = \frac{I_0/I}{1 + j\omega(CV_T/I)}. \tag{36}$$

Consider an input of the form

$$u(t) = I_{cu} + I_{pu} \cos(\omega t). \tag{37}$$

Using (36), we obtain for the noiseless case

$$y(t) = I_{cy} + I_{py} \cos(\omega t + \phi) \tag{38}$$

where

$$I_{cy} = H(0) I_{cu} = \frac{I_0}{I} I_{cu} \tag{39}$$

$$I_{py} = |H(j\omega)| I_{pu} = \frac{I_0/I}{\sqrt{1 + \omega^2 (CV_T/I)^2}} I_{pu} \tag{40}$$

$$\phi = \angle H(j\omega) = -\tan^{-1}(\omega(CV_T/I)). \tag{41}$$

From (12), (32), and (38) we have

$$\mu(t) = f'(v(t)) = \frac{y(t)}{V_T} = \frac{I_{cy}}{V_T} + \frac{I_{py}}{V_T} \cos(\omega t + \phi). \tag{42}$$

This can be used in (29) to calculate η. The result is

$$\eta = \frac{1}{V_T^2} \left(I_{cy}^2 + \frac{1}{2} I_{py}^2 \right). \tag{43}$$

A related result for this special case is given in [18] and [19].

In order to obtain some intuition about these calculations, notice that, if the input were a dc signal and the circuit were in steady state, the noise PSD at the output would be the PSD of the noise across the capacitor times g_m^2, where g_m is the transconductance of Q_4 at the operating point. Here, instead, the parameter involved is $\mu(t)$ which, from (42), can be seen to be the *instantaneous transconductance*, $g_m(t)$, which varies with the signal. From (29), then, it is seen that η is nothing but the average of $g_m^2(t)$ over the period of the input.

In order for Q_1 in Fig. 5 not to turn off, the circuit must operate in class A with $I_{pu} < I_{cu}$ in (37). This means that η can vary by at most a factor of 1.5 from the "no signal" to the "full signal" condition. Thus, the variation of noise with signal for this circuit is not strong. A much more dramatic variation can be observed in class-AB or class-B circuits, where signal currents can become much larger than

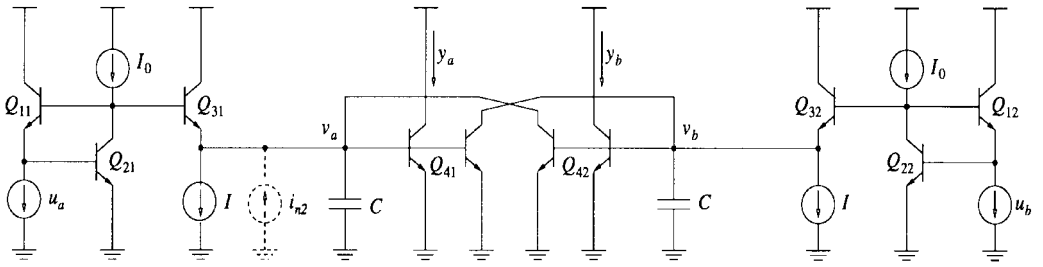

Fig. 6. First-order class-B log-domain circuit.

quiescent currents. Such a circuit is shown in Fig. 6 [2], [16], where u_a and u_b are the input currents, y_a and y_b are the output currents, and the current i_{n2} represents noise. Though this is a balanced structure, and does not fit exactly into the discussion above, the analysis presented can still be applied, although it is mathematically more involved and contains certain approximations. Such an analysis is given in the Appendix, and leads to the conclusion that, when u_a and u_b are alternate half cycles of a sinewave (so that the difference $u_a - u_b$ is sinusoidal), (30) and (31) are valid with

$$\eta \approx \frac{1}{2IV_T^2}\int_0^T |y(t)|^2\,dt \tag{44}$$

where $y(t) = y_a(t) - y_b(t)$ is the differential output current in absence of noise. Therefore, when u_a and u_b are half sine waves with amplitude I_{pu}, the value of η becomes

$$\eta = \frac{I_{py}^2}{4V_T^2} \tag{45}$$

where I_{py} is given by (40). The result in (45) should be compared to (43). Due to the absence of the dc term in this expression, the noise, through η, can vary drastically with the amplitude of the signal.

From (45), it can be seen that the signal dependent term in the expression for the PSD of the output noise (31) is in fact directly proportional to the output signal power, resulting in a constant signal to noise ratio. Integrating (31) over an interval $[\omega_l, \omega_u]$, the output noise power can be obtained as

$$N = \eta\,\frac{k^2}{2\pi a}\,(\tan^{-1}(\omega_u/a) - \tan^{-1}(\omega_l/a))S_2. \tag{46}$$

From (35), it can be seen that $S_2 = S_i V_T^2/I_0^2$, where S_i is the PSD of the noise current i_{n2} in Fig. 6. Using this and (45) in (46), and recognizing that the output signal power is $I_y^2/2$, leads to the following expression for the signal-to-noise ratio:

$$\frac{S}{N} = \frac{2I_0^2}{S_i\left(\dfrac{k^2}{2\pi a}\right)(\tan^{-1}(\omega_u/a) - \tan^{-1}(\omega_l/a))}. \tag{47}$$

VI. Experimental Results

Measurements were performed on the circuits of Figs. 5 and 6 implemented with discrete components using $I_0 = 20\ \mu$A, $I = 20\ \mu$A. These values result in $k = a = 2\pi\times 12.3$ krad/s. A stationary noise current i_{n2} was injected, and was deliberately made large in order to dominate all other noise in the circuit and enable a comparison to the analytical results. The output current was converted to a voltage using a transresistance amplifier, and the noise was measured using a spectrum analyzer. The experiments performed are described below.

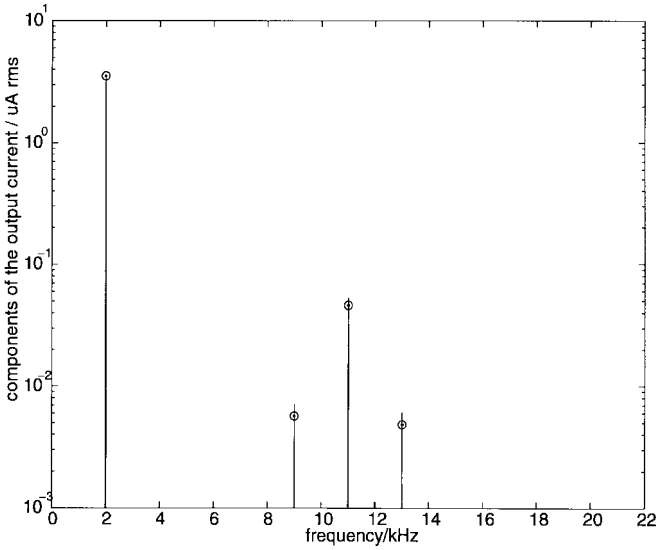

Fig. 7. Intermodulation components due to deterministic interference. Lines: calculated spectrum; circles: measured values.

1) Class-A circuit (Fig. 5):
   - A sinusoidal interference of $0.1\ \mu\text{A}\cos(2\pi \times 11\text{ kHz} \times t)$ was injected. The input to the filter was $20\ \mu\text{A} + 5\ \mu\text{A}\cos(2\pi \times 2\text{ kHz} \times t)$. From the equivalent circuit of Fig. 4(b), the intermodulation components were calculated. The calculated values and the measured points are indicated on Fig. 7.
   - White noise with a PSD of 0.35 nA/$\sqrt{\text{Hz}}$ was injected as shown in Fig. 5. The input to the filter was $20\ \mu\text{A} + 5\ \mu\text{A}\cos(2\pi \times 6\text{ kHz} \times t)$. Using (31), (39), (40), and (43) the output noise PSD was calculated. The calculated curve and the measured points are shown in Fig. 8.
2) Class-B circuit (Fig. 6):
   - A noise current with a PSD of 0.35 nA/$\sqrt{\text{Hz}}$ was injected as in Fig. 6. The output noise PSD was calculated using ((31), (40), and (45). The calculated curves and measured points are shown in Fig. 9. It is apparent that the noise increases with an increase in the signal.
   - In order to verify that the signal-to-noise ratio is a constant as described by (47), the output noise

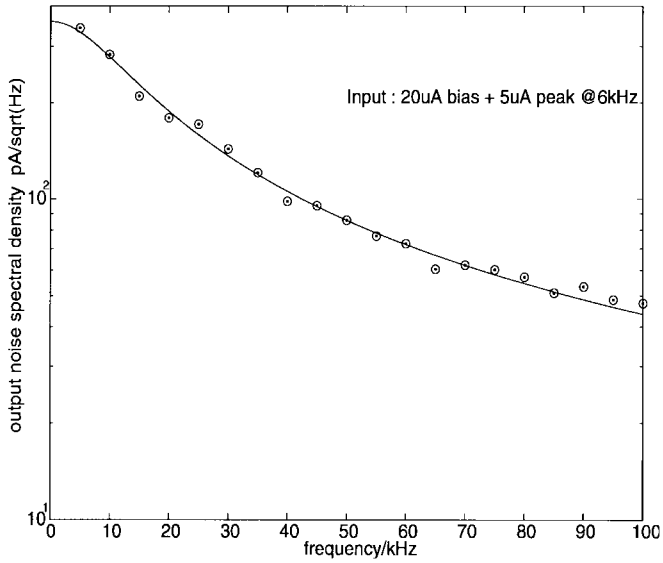

Fig. 8. Output noise current spectral density for the class-A circuit. Lines: calculated spectrum; circles: measured values.

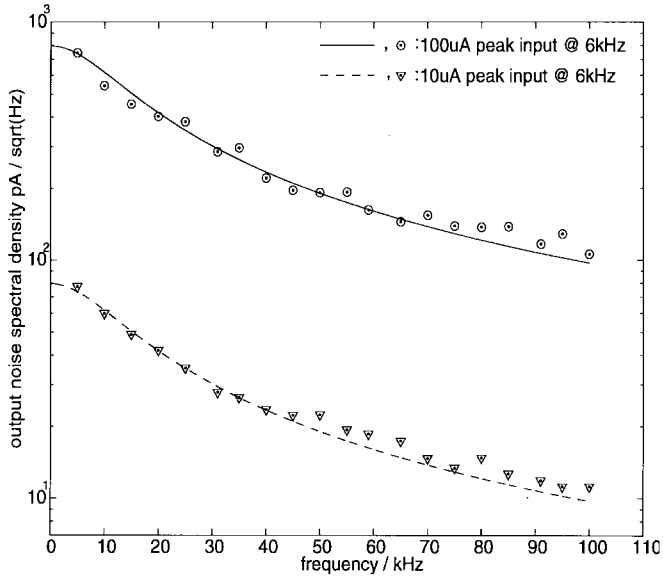

Fig. 9. Output noise current spectral density for the class-B circuit at two different current levels. Lines: calculated spectrum; circles: measured values.

in a 0–100-kHz band was measured for different signal levels with white noise injected as above. The measured points, along with the value calculated from (47), are shown in Fig. 10.

VII. Conclusions

Conventional techniques, used for the analysis of noise in linear circuits, cannot be used for companding signal processors. This is because the latter, although externally linear, exhibit nonlinear behavior between internal points and the output. Certain appropriate techniques for the analysis of noise and small interference in companding signal processors have been discussed. Explicit relations were given for the case of stationary white noise with a periodic input. It is found that,

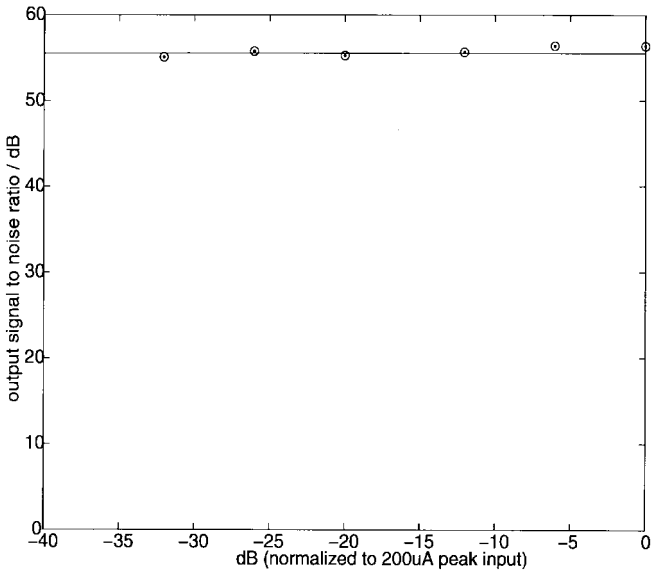

Fig. 10. Output signal to noise (0–100-kHz band) ratio. Lines: calculated spectrum; circles: measured values.

in general, the output noise of such systems depends on the input signal amplitude and signal shape. Log-domain circuits were considered as examples and the theoretical predictions were found to agree with experiments.

Appendix

In the appendix, the subscript $_2$ will be added to the variables that are influenced by the presence of noise i_{n2}. When we consider the circuit in the absence of noise, the subscript $_2$ will be dropped. Using k and a given by (33) and (34), respectively, a straightforward analysis of the circuit in Fig. 6 results in

$$\frac{d}{dt}\,y_{a2} = ku_a - ay_{a2} - \frac{1}{CV_T}\,y_{a2}y_{b2} + \frac{1}{CV_T}\,y_{a2}i_{n2} \quad (48)$$

$$\frac{d}{dt}\,y_{b2} = ku_b - ay_{b2} - \frac{1}{CV_T}\,y_{a2}y_{b2}. \quad (49)$$

We define the differential input signal $u(t)$ and differential output signal (including the noise) by

$$u(t) = u_a(t) - u_b(t) \quad (50)$$

$$y_2(t) = y_{a2}(t) - y_{b2}(t). \quad (51)$$

Using $f(v)$ and n_2 given by (32) and (35), respectively, we get from (48) to (51)

$$\frac{d}{dt}\,y_2 = -ay_2 + ku + kf'(v_a)n_2 \quad (52)$$

where the approximation $f'(v_{a2}) \approx f'(v_a)$ has also been used. If $i_{n2} = 0$, (52) reduces to (2) and (3). Hence, the overall circuit is externally linear with a transfer function given by (36). Defining the output noise n_{o2} in the same way as in the first relationship of (22) ($n_{o2} = y_2 - y$) when $i_{n2} \neq 0$, and comparing (52) with (18) and (19) we can state that (24) is

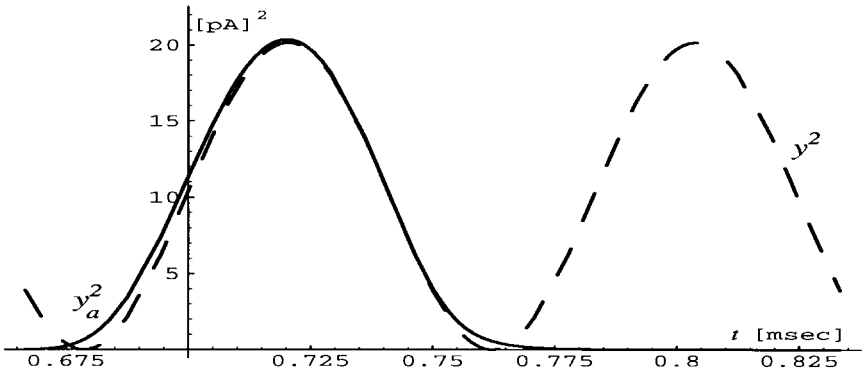

Fig. 11. Numerical solution for $y_a^2(t)$ (solid line) in the nonlinear differential equations (54) and (55) and for $y^2(t)$ (dashed line) where $u_a(t)$ and $u_b(t)$ are, respectively, the positive and negative half cycles of $u(t)$ where $u(t)$ is given by (37). The numerical values are: $k = a = 76\,923$ rad/s, $I_{pu} = 20\ \mu$A, and $\omega = 2\pi \times 6000$ rad/s.

still valid with

$$\mu(t) = f'(v_a(t)) = \frac{1}{V_T}\, y_a(t) \tag{53}$$

instead of (42). Thus if the (differential) input is given by (37), then all the formulas in (38)–(41) are still valid. However, for calculating $\mu(t)$ in (53) $y_a(t)$ has to be found from the following nonlinear differential equations [see (48) and (49)]:

$$\frac{d}{dt}\, y_a(t) = k u_a(t) - a y_a(t) - \frac{1}{CV_T}\, y_a(t) y_b(t) \tag{54}$$

$$\frac{d}{dt}\, y_b(t) = k u_b(t) - a y_b(t) - \frac{1}{CV_T}\, y_a(t) y_b(t). \tag{55}$$

In addition, the *single-ended* input currents u_a and u_b have also to be known for computing $\mu(t)$ in (53). We assume that u_a and u_b consist of the positive and negative half-cycles of $u(t)$, respectively, as in [16]. Then a detailed analysis of the circuit in Fig. 6 shows that the differential output current y is supported mostly by the left part of the circuit (Q_{11}, Q_{21}, Q_{31}, and Q_{41}) while the right part of the circuit (Q_{12}, Q_{22}, Q_{32}, and Q_{42}) is practically turned off for $y > 0$, and vice versa when $y < 0$. This simplified view leads to an approximation which is appropriate for computing η in (29) in terms of $\mu^2 = (y_a/V_T)^2$ [see (53)]. For a sinusoidal (differential) input an illustration is shown in Fig. 11. The single-ended $y_a(t)$ has been obtained by solving (54) and (55) numerically based on the values shown in the caption of Fig. 11, while $y(t)$ has been computed using (38)–(41). It is seen that the two functions are very similar in the interval $[0, T/2]$. Thus, a reasonable approximation can be given for η in (29) and (53) as follows:

$$\eta = \frac{1}{TV_T^2} \int_0^T y_a^2(t)\, dt \approx \frac{1}{TV_T^2} \int_0^{T/2} y^2(t)\, dt. \tag{56}$$

In particular, when $u(t)$ is a sinusoid given by (37) with $I_{cu} = 0$, (56) simplifies to

$$\eta = I_{py}^2 / 4V_T^2. \tag{57}$$

ACKNOWLEDGMENT

The authors thank G. Efthivoulidis and the reviewers for their comments on the manuscript.

REFERENCES

[1] Y. P. Tsividis, V. Gopinathan, and L. Tóth, "Companding in signal processing," *Electron. Lett.*, vol. 26, pp. 1331–1332, Aug. 1990.
[2] E. Seevinck, "Companding current-mode integrator: A new circuit principle for continuous-time monolithic filters," *Electron. Lett.*, vol. 26, pp. 2046–2047, Nov. 1990.
[3] R. W. Adams, "Filtering in the log domain," presented at the 63rd Audio Engineering Society Conf.. New York, May 1979, preprint 1470.
[4] M. Banu and Y. Tsividis, "Fully integrated active *RC* filters," in *Proc. 1983 ISCAS*, May 1983, pp. 602–605.
[5] D. R. Frey, "A general class of current mode filters," in *Proc. IEEE 1993 ISCAS*, Chicago, IL, May 1993, pp. 1435–1438.
[6] Y. Tsividis, "Externally linear, time-invariant systems and their application to companding signal processors," *IEEE Trans. Circuits Syst. II*, vol. 44, pp. 65–85, Feb. 1997.
[7] L. A. Zadeh and C. A. Desoer, *Linear System Theory: The State Space Approach.* New York: McGraw-Hill, 1963.
[8] S. O. Rice, "Response of periodically varying systems to shot noise-application to switched RC circuits," *Bell Syst. Tech, J.*, vol. 49, no. 9, pp. 2221–2247, Nov. 1970.
[9] A. Demir, E. W. Y. Liu, and A. L. Sangiovanni-Vincentelli, "Time-domain non-Monte Carlo noise simulation for nonlinear dynamic circuits with arbitrary excitations," *IEEE Trans. Computer-Aided Design*, vol. 15, pp. 493–505, May 1996.
[10] T. Ström and S. Signell, "Analysis of periodically switched linear circuits," *IEEE Trans. Circuits Syst.*, vol. CAS-24, pp. 531–541, Oct. 1977.
[11] L. Tóth and K. Suyama, "Exact noise analysis of ideal SC networks," in *Proc. 1991 IEEE ISCAS*, Singapore, June 1991, pp. 1585–1588.
[12] T. A. C. M. Claasen and W. F. G. Mecklenbräuker, "On stationary linear time-varying systems," *IEEE Trans. Circuits Syst.*, vol. CAS-29, pp. 169–184, Mar. 1982.
[13] R. G. Meyer, "Noise in transistor mixers at low frequencies," *Proc. Inst. Elect. Eng.*, vol. 114, no. 5, pp. 611–618, May 1967.
[14] M. Okumura, H. Tanimoto, T. Itakura, and T. Sugawara, "Numerical noise analysis for nonlinear circuits with periodic large signal excitation including cyclostationary noise sources," *IEEE Trans. Circuits Syst. I*, vol. 40, pp. 581–590, Sept. 1993.
[15] J. Roychowdhury and P. Feldmann, "A new linear-time harmonic balance algorithm for cyclostationary noise analysis in RF circuits," in *Proc. Asia and South-Pacific Design Automation Conf.*, Chiba, Japan, Jan. 1997, pp. 483–492.
[16] F. Yang, C. Enz, and G. van Ruymbeke, "Design of low-power and low voltage log-domain filters," in *Proc. 1996 IEEE ISCAS*, Atlanta, GA, May 1996, pp. 117–120.
[17] D. R. Frey, "Exponential state space filters: A generic current mode design strategy," *IEEE Trans. Circuits Syst. I*, vol. 43, pp. 34–42, Jan. 1996.

[18] M. Punzenberger and C. Enz, "A 1.2 V BiCMOS class-AB log-domain filter,"in *Dig. 1997 ISSCC*, San Francisco, CA, Feb. 1997, pp. 56–57; also slide supplement, p. 34.
[19] J. Mulder, M. H. L. Kouwenhoven, and A. H. M. van Roermund, "Signal × noise intermodulation in translinear filters," *Electron. Lett.*, vol. 33, pp. 1205–1207, July 1997.

László Tóth was born in Budapest, Hungary, on March 25, 1957. He received the M.Sc. and the Candidate's (Ph.D.) degrees from the Technical University of Budapest, Budapest, Hungary, and the Hungarian Academy of Sciences, in 1982 and 1987, respectively.

During 1982–1993, he was with the Research Institute for Telecommunications (TKI), dealing with digital filtering, analysis of switched capacitor networks and speech compression. Since 1993, he has been with the Technical University of Budapest. During 1989–1990 and 1995–1996 he was with the MAD–VLSI Laboratory and the Microelectronic Circuits and Systems Laboratory, respectively, Columbia University, New York, dealing with noise performance of active *RC* filters, switched-capacitor networks, and nonlinear circuits. In 1997, he spent seven months with Bell Laboratories, Murray Hill, NJ, working on companding signal processors and sigma–delta data converters.

Yannis P. Tsividis (S'71–M'74–SM'75–F'86), for a photograph and biography, see this issue, p. 1187.

Nagendra Krishnapura received the B.Tech. degree in electronics and communication engineering from the Indian Institute of Technology, Madras, India, in 1996.

Since September 1996 he has been a Research Assistant in the Microelectronic Circuits and Systems Laboratory at Columbia University, New York, where he is investigating companding filters for signal processing. He spent the summers of 1997 and 1998 with Texas Instruments IncorporatedLucent technologies, working on companding filters and high speed synthesizers, respectively.